

## Technological implications of neo-formed hematite crystals in ceramic lead glazes

Roberta Di Febo <sup>a</sup>, Judit Molera <sup>a</sup>, Trinitat Pradell <sup>b</sup>, Oriol Vallcorba <sup>c</sup> and Claudio Capelli <sup>d</sup>

<sup>a</sup>MECATMAT Research Group Engineering Department, Faculty of Sciences and Technology, University of Vic – Central University of Catalonia, Barcelona, Spain; <sup>b</sup>Physics Department, Barcelona Research Center in Multiscale Science and Engineering (BRCMSE), Universitat Politècnica de Catalunya, Barcelona, Spain; <sup>c</sup>Alba Synchrotron Light Source, Barcelona, Spain; <sup>d</sup>Università degli Studi di Genova, Genova, Italy

### ABSTRACT

Hexagonal neo-formed crystallites have been observed in thin section of different medieval and post-medieval lead-glazed ceramics. Although they are clearly visible in thin section using plane polarized light, their plate shape makes them barely seen on the polished cross sections. Basal sections have never been found on the polished sections and only few transversal very thin sections could be seen. In this case, the morphology resembles acicular and it is not possible to analyze them properly by SEM–EDX because the crystals are very thin and the glaze surrounding is analyzed as well. Micro-Raman microscopy was carried out directly on the polished thin sections. This technique allows specific areas as small as 1  $\mu\text{m}$  in diameter to be analyzed and it is able to characterize inclusions that are not found on the glaze surface. However, the wavenumber features observed cannot be assigned to a specific compound. The thickness of the crystallites (a few hundred nanometers) seems to be responsible for the low sensitivity of the Raman instrumentation.  $15 \times 15 \mu\text{m}^2$  micro-X-ray diffraction patterns using synchrotron radiation (SR- $\mu\text{XRD}$ ) in transmission geometry were obtained from the crystals using the same thin section preparation. SR- $\mu\text{XRD}$  was able to localize the crystallites and avoid the overlapping signals corresponding to other mineral phases. In this way, the hexagonal crystallites present in the glaze have been unambiguously identified as hematite crystallites. Finally, some replications were made under laboratory-controlled conditions to determine the firing conditions in the formation of those crystallites. The presence of hematite coexisting with melanotekite indicates a firing temperature  $<925^\circ\text{C}$ , while the presence of only hematite suggests a firing temperature  $>925^\circ\text{C}$ .

### ARTICLE HISTORY

Received 9 May 2017  
Accepted 14 December 2017

### KEYWORDS

Hematite; ceramic lead glazes; OM; SEM–EDS; micro-Raman; SR- $\mu\text{XRD}$

## 1. Introduction

Studying lead-glazed potteries from different places and periods by thin section petrography, we found brown/deep orange hexagonal neo-formed crystallites precipitated at the body–glaze interface (Figure 1(a, b)). We documented these kinds of crystallites in green-glazed wares from North Africa (Figure 1(c)) and Italy (thirteenth century), Spanish-glazed coarse wares (eighteenth century), Ligurian Taches Noires wares (eighteenth century), Catalan and French imitations (Figure 1(d)) of the Ligurian Taches Noires wares (eighteenth–nineteenth century) and Catalan coarse-glazed wares (eighteenth century), (Capelli, Mannoni, and Cabella 2007; Capelli et al. 2013; Beltrán de Heredia Bercero et al. 2015; Gómez et al. 2015; Di Febo 2016; Capelli et al. 2017). The medieval and post-medieval lead-glazed ceramics taken into account for our study share some common technical features. All the ceramics exhibit a red/orange color of the bodies due to oxidizing firing conditions and an interface moderately developed. The ceramic bodies consist of Fe-rich

clay while the glazes are of the transparent high lead type (Tite et al. 1998). They contain between 45 and 60% PbO, an alkali content normally lower than 2% ( $\text{Na}_2\text{O} + \text{K}_2\text{O}$ ), an alumina content in the range 2–7%  $\text{Al}_2\text{O}_3$  and an iron oxide content of about 4.5–6% (FeO wt%).

These crystallites are clearly visible in thin section with plane polarized light (PPL). This is due to the fact that petrographic inspection of the glaze thin sections gives a 3D perspective of the crystallites and is able to reveal their microstructural features and distribution in the glazes. On the contrary, the plate shape makes them barely seen on the polished cross sections using scanning electron microscopy (SEM). Consequently, if they are not recognized, it is very unlikely that they can be analyzed. The basal sections have never been found on the polished surfaces and only few transversal very thin sections could be seen. In this case, it is not possible to analyze them properly by SEM–EDX because the sections of the crystallites are thinner than the electron beam. In order to identify

the hexagonal crystallites, additional data from micro-Raman spectroscopy and synchrotron radiation micro-X-ray diffraction (SR- $\mu$ XRD) were obtained using thin section preparation.

The use of Raman microscopy for identifying and studying archaeological materials has flourished in recent years in addition to the standard analytical techniques (De Faria, Silva, and de Oliveira 1997; Clark and Curri 1998; Smith and Clark 2001; De Faria and Lopes 2002; Colomban and Truong 2004; Casadio, Daher, and Bellot-Gurlet 2016; Howell, Edwards, and Vandnabeele 2016). Some advantages of the Raman microscopy include its molecular specificity, no destructiveness, high spatial and spectral resolution and *in situ* analysis. In the Raman microscopy, materials are identified by comparing their characteristic vibrational spectra with those in a database. In our case, we work directly on the polished thin sections of the samples, because we consider that it is extremely important to see and check the crystallites on which the analysis is performed. In addition,  $\mu$ XRD using synchrotron radiation patterns have been also acquired on the thin glaze sections. The advantage of using synchrotron light is the high brilliance and probe size spot of some tens of micrometers. Other benefits include the possibility to localize the crystallites even if they are not found on the glaze surface layer and to avoid the overlapping signals corresponding to other crystallites. In this way, the hexagonal crystallites present in the glaze have been identified. Once the nature of these crystallites was identified, replications were made in controlled laboratory conditions in order to determine the temperature and firing conditions for their formation.

## 2. Experimental

A French imitation of the Ligurian Taches Noires pottery from the workshop of Jouques (Provence, France) has been analyzed in order to identify the hexagonal crystallites. We choose this sample due to the abundance of large hexagonal crystallites, some of them larger than 50  $\mu\text{m}$ . The sample 9703 (Figure 1(d)) selected for the combined analyses is dated from the first half of the nineteenth century and corresponds to a plate. According to written sources, the workshop of Joques was established by an Italian, possibly a Ligurian potter (Amouric and Vallauri 1993). The ware called Taches Noires was developed in Albisola (Liguria, NW Italy) during the eighteenth century (Cameirana 1970, 1977). This type of ware is characterized by a fine, hard, deep red fabric and transparent glazes decorated with wavy dark bands of manganese oxides (Blake 1981).

The crystallites were first studied by optical microscopy (OM) using a petrological microscope (LEICA DM 2700 P). All of the stages of the analysis were carried out on the same polished thin section.

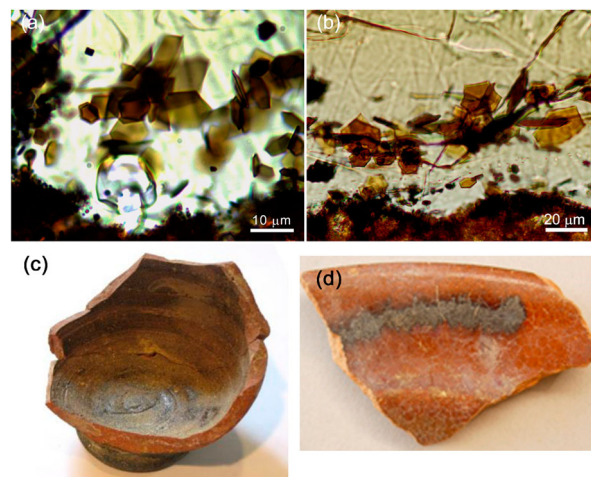


**Figure 1** (a) and (b) OM images in PPL. Hexagonal crystallites in the glaze-body interface of a green-glazed ware and of a Ligurian Taches Noires pottery are visible. (c) Green-glazed ware from North Africa (thirteenth century). (d) French imitation of the Ligurian Taches Noires ware (eighteenth-nineteenth century).

In this manner, we were able to constantly observe and analyze the same inclusions. The ceramic sample was ground down to a standard thickness of 30  $\mu\text{m}$  that permits the growth habits of the micro-crystallites to be identified by OM observation at magnifications ranging from about 10 $\times$  to 100 $\times$ . Details of thin section preparation methods can be found in Poole and Sims (2015). The crystallites as well as the glaze were analyzed by scanning electron microscopy with an energy-dispersive x-ray spectroscope attached (SEM-EDS) to ascertain their chemical composition. The bulk chemical composition of the glaze was determined by analyzing areas and avoiding the glaze-body interface, as well as other crystallites. A crossbeam workstation (Zeiss Neon 40) equipped with SEM (Shottky FE) column and EDS (INCAPentaFETx3 detector, 30 mm<sup>2</sup>, ATW2 window) was employed. The microscope was operated at 20 kV, with 100 s measuring times, and backscattered electron (BSE) images were obtained. Quantitative analysis calibration was accomplished with mineral and glass standards.

Focus ion beam (FIB) was used to produce polished cross sections of the crystallites. A crossbeam workstation (Zeiss Neon 40) equipped with SEM (Shottky FE) and Ga + FIB columns was used to prepare cross sections of the crystals. First, the sample surface was coated with a thin protective Pt layer (1  $\mu\text{m}$ ) by ion-beam-assisted deposition; then the cross section was cut and polished and a thin layer of Pt deposited to enhance conductivity. Subsequently, secondary electron SEM images of the inclusions were obtained at 5 kV.

Micro-Raman analyses were carried out directly on the polished thin sections of the glazes at the Centres Científics i Tecnològics, University of Barcelona. Spectra were obtained with a HORIBA Jobin Yvon

LabRam HR 800 dispersive spectrometer, equipped with an Olympus BXFM optical microscope, using a 600 g/mm grating and a Synapse CCD detector cooled at  $-70^{\circ}\text{C}$ . The Raman spectra reported in this study were recorded with the 532 nm excitation line of a solid state laser.

SR- $\mu$ -XRD was performed on the focused-beam station of the beamline BL04<sup>12</sup> at the ALBA Synchrotron. The areas of interest from the polished thin sections were selected using an on-axis visualization system and measured in transmission geometry with a focused beam of  $15 \times 15 \mu\text{m}^2$  (full width at half-maximum). The energy used was 29.2 keV ( $\lambda = 0.4246 \text{ \AA}$ ) and the diffraction patterns were recorded with a Rayonix SX165 CCD detector (active area of 165 mm diameter, frame size  $2048 \times 2048$  pixels,  $79 \mu\text{m}$  pixel size, dynamic range 16 bit). The calibration of the sample to detector distance and beam center (from a LaB<sub>6</sub> sample measured at the same conditions) and the radial integration of the images were performed with the Fit2D software.

Individual crystallites were measured at different rotation angles relative to a vertical axis centered on the crystal. The total oscillation ranges from  $-30^{\circ}$  to  $30^{\circ}$  with each of the diffraction images comprising  $10^{\circ}$  oscillation. The radial integration of each image, although is not producing a powder pattern (missing reflections and intensities only from a single grain), contains enough peaks to identify the possible phases. Identification of the compounds has been performed based on the Powder Diffraction File (PDF) database from the International Centre for Diffraction Data (ICDD).

Reproductions of glazes, with the same composition than that of the sample 9703, were fired in oxidizing conditions at different temperatures;  $850^{\circ}\text{C}$ ,  $900^{\circ}\text{C}$ ,  $920^{\circ}\text{C}$ ,  $950^{\circ}\text{C}$ ,  $980^{\circ}\text{C}$  and  $1020^{\circ}\text{C}$ . The thermal paths were similar in all cases, 6 h of heating ramp, 10 min at maximum temperature and free cooling into the electric kiln. Samples were analyzed by OM and SEM.

### 3. Results

The sample 9703, selected for the combined analyses, corresponds to a nineteenth-century French imitation of Ligurian *Taches Noires* ware from Joques (Provence, France). This type of ware is characterized by transparent brown glazes decorated with wavy dark bands of manganese oxides (Blake 1981). The chemical composition of the sample 9703 shows high PbO (54.4 wt%) and SiO<sub>2</sub> (35.2 wt%) content, lower amounts of Fe<sub>2</sub>O<sub>3</sub> (4.6 wt%), Al<sub>2</sub>O<sub>3</sub> (2.5 wt%), MnO (0.8 wt%), CaO (0.7 wt%), MgO (0.3 wt%) and very low Na<sub>2</sub>O and K<sub>2</sub>O content (0.2 wt% and 0.9 wt%, respectively). The MnO content suggests that the manganese used for the dark decoration was partly dissolved into the glaze.

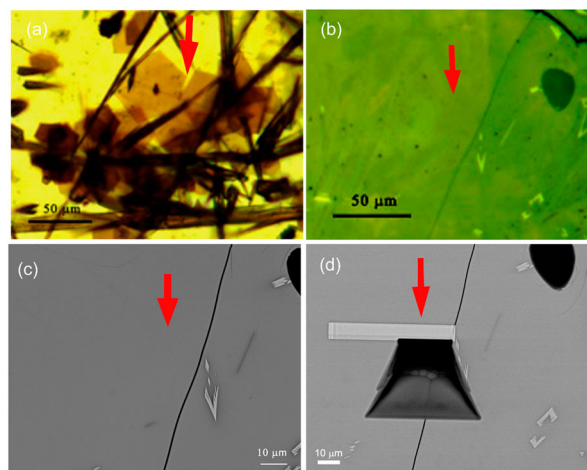


**Figure 2.** (a) OM image in plane polarized light of the thin section of the glaze 9703 (PPL). Hexagonal crystals (red arrow) in association with elongated honey skeletal crystals are clearly visible (b) The same area as in picture (a) in reflected light. Red arrow indicates the position of the hexagonal crystal marked on (a). It is not on the glaze surface and then it is not visible by reflection mode. (c) SEM backscattering image of the same area as in picture (a). The red arrow indicates the place of the same hexagonal crystal marked in (a). (d) SEM image of FIB polished cross section in the area of the hexagonal crystallite.

Two types of crystallites are found in the thin section of the glaze: elongated honey skeletal crystals and hexagonal brown/orange crystals (Figure 2(a)). The first ones were identified as melanotekite (Pb<sub>2</sub>Fe<sub>2</sub>-Si<sub>2</sub>O<sub>9</sub>) formed during the firing process from the reaction among the constituents of the glaze mixture (Figure 3; Di Febo et al. 2017). Melanotekite crystals are easily seen in reflected light and in SEM backscattering mode as light crystals. On the contrary, the hexagonal crystallites are not found on the polished glaze surface and only a few very thin cross sections of these are visible (Figure 2(b,c)). They exhibit a light tinge in reflected light and grayish color in BSE images. In the area of the hexagonal crystallites of Figure 2(a) a

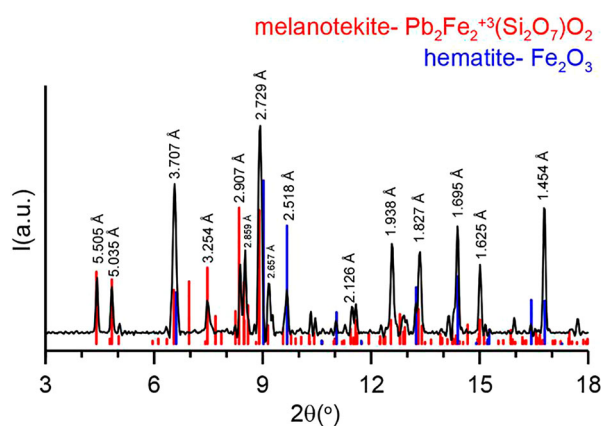


**Figure 3.** XRD pattern of melanotekite crystals. The references patterns marked correspond to the JCPDF database patterns 00-020-0585 for melanotekite and 01-079-1741 for hematite.

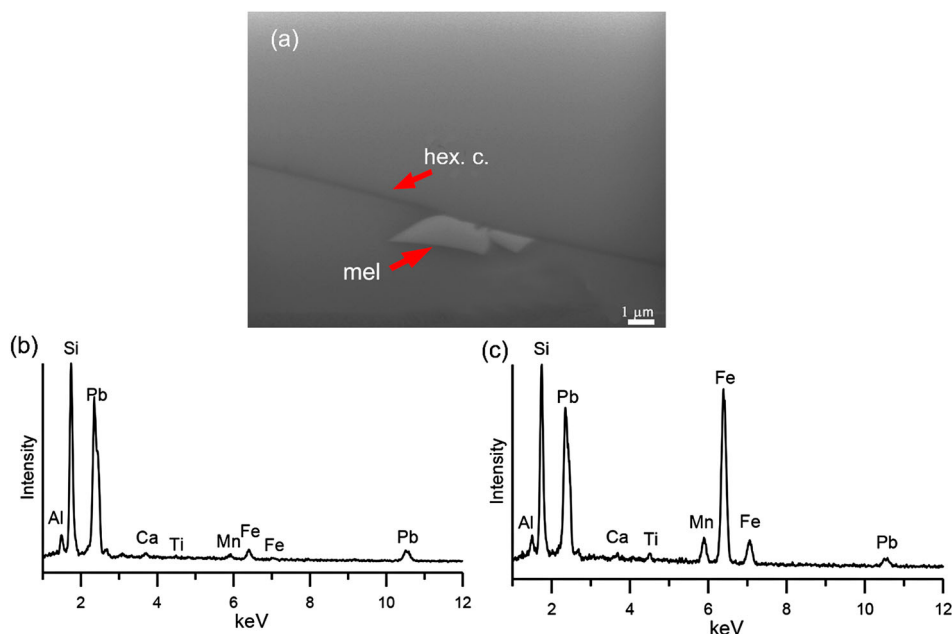


**Figure 4.** (a) SEM image of FIB polished cross-section cut through a hexagonal crystallite. A very thin laminar section of hexagonal crystallite (hex.c.) and a crossed crystal of melanotekite (mel, bright contrast) can be observed. (b) EDS analysis on the glaze surface. (c) EDS analysis on the laminar section of the hexagonal crystallite.

26 × 40 μm cross section was polished by FIB and observed using the secondary electrons (Figure 2(d)). Figure 4(a) shows the FIB polished cross-section cut through the hexagonal crystallites. From the FIB cross-section images, it is seen that the hexagonal crystallite was mostly found at a depth of about 20 μm in respect to the glaze preparation and that its thickness is about of 250 nm. The EDS analysis on the cross sections of the hexagonal crystallites is difficult because they are smaller than the electron beam probe volume. However, spectra from the cross sections of the hexagonal crystallites and from the glaze surface were obtained (Figures 4(b,c)). When we compare the spectra, we can see that the most remarkable difference is due to the iron content, which is very high in the spectrum of the cross sections of the crystallites. In addition, the crystallites were richer in Mn than the glaze. The Mn was found dissolved in the glaze and its presence is related to the dark decoration. As the crystallites are planar and oriented in the three dimensions, we did not manage to cut the crystallites to observe and analyze the basal sections.

In the next step, the hexagonal crystallites were subjected to Raman analysis. The optical microscope coupled with the Raman spectrometer permits hexagonal crystallites to be examined at high magnification and allows specific areas as small as 1 μm in diameter to be analyzed. In this instance, we took advantage of Raman microscopy that is able to provide analyzing inclusions that are not found on the glaze surface. We can defocus the image through the focus knob until the hexagonal crystallites are visible on the top of the glaze layer and analyze them. Figure 5(a,b) refers

to the spectra acquired on the glaze surface and on the singular crystallite, respectively. When we compare the two spectra, we can see that the instrumentation is not sensitive enough. A wavenumber feature at about 689.5 cm<sup>-1</sup> can be clearly observed and possibly another at about 1320 cm<sup>-1</sup>. We have acquired different spectra on the hexagonal crystallites changing the laser power (0.5; 0.05; 1.5; 2 and 5.5 mW) and the laser wavelength (632 nm), but the presence of a specific phase cannot be confirmed based on the wavenumber features observed.

In addition, we also analyzed the thin cross sections rising on the glaze surface. Again, we were not able to

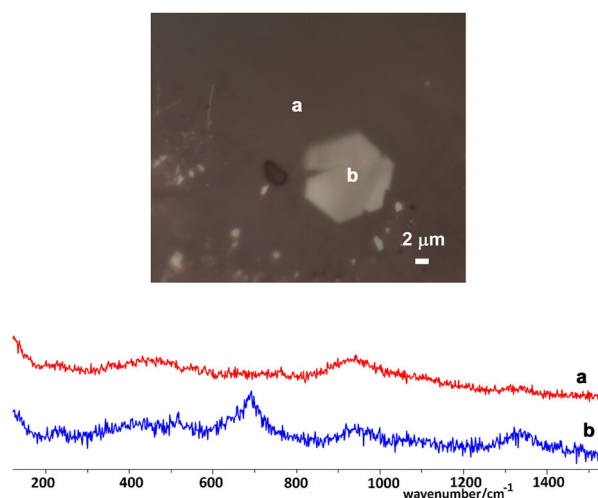


**Figure 5.** Above: Raman image of a hexagonal crystallite. Below: Raman spectra acquired on the glaze surface (a) and on the hexagonal crystallite (b). (Laser power: 2 mW; accumulation time: 5 s; number of accumulation: 10; objective magnification: 100×).

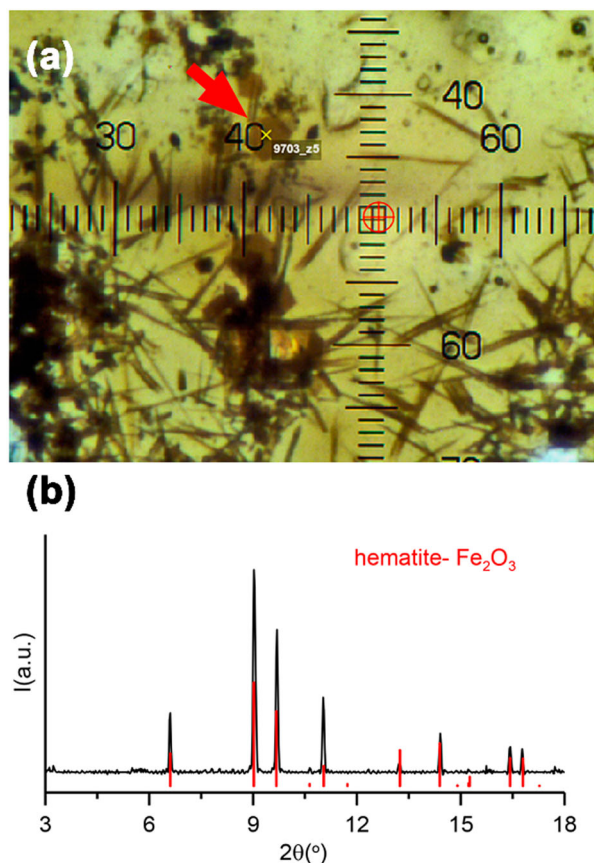


**Figure 6.** (a) Photomicrograph of the thin section of the sample 9703 from the Synchrotron camera. The hexagonal crystallites are clearly visible and the analysis spot (9703-z5) is shown in the picture. (b) XRD pattern of the crystal analyzed. The reference pattern marked corresponds to the JPDF database pattern 01-079-1741 for hematite.

determine any specific compound and a characteristic feature at about  $625.2\text{ cm}^{-1}$  was observed.

Following this, a Micro-X-ray diffraction in transmission geometry using Synchrotron Light was performed directly on the polished thin section of the sample 9703 (Figure 6(a)). The advantage of using thin section is that the crystallites could be easily localized in the glaze, even if they were not found on the glaze surface layer. The  $15\text{ }\mu\text{m} \times 15\text{ }\mu\text{m}$  spot allowed to measure individual crystallites. The data obtained show unambiguously that the hexagonal phase corresponds to hematite (Figure 6(b)). We can also ascertain that the presence of Mn determined by SEM do not affect the lattice spacing and consequently the position of the hematite reflections. We can conclude that Mn is not substituting iron in the structure of hematite, but probably acted as a nucleation agent. We can highlight that the hematite crystallites often show a visible feature at the center.

#### 4. Discussion

Hematite crystals are the principal mineral phase found in the Fe-rich glazes fired in oxidizing conditions (Dakhai, Orlova and Mikhailenko 1999). Nevertheless,

the case study presented demonstrates the difficulty of identifying this type of crystallites in ceramic lead glazes using the most common routine analytical techniques. We observe two basic problems. The first one is the thickness (a few hundred nanometers) of the crystallites, which is probably responsible for the low sensitivity of the Raman instrumentation. In this way, the wavenumber features observed cannot be assigned to a specific mineral phase. The second one is the arrangement of these crystals in the glaze. Most of them were found at a depth of about  $20\text{ }\mu\text{m}$  with respect to glaze preparation. The basal sections were never observed neither in the BSE nor in FIB cross-section images. Then, the work of thin section petrography is crucial to connect the hexagonal habit of these crystals to the thin cross sections observed in the SEM, to situate their distribution in the glaze matrix and analyze them by SR- $\mu$ -XRD.

The hematite micro-crystallites are formed in the glaze-body interface from the reaction between the components of the glaze mixture and the ceramic paste. During the cooling, the capacity of the melt to retain the Fe in solution is lessened and the excess is precipitated as thin plate crystals (Fraulini 1933). According to the literature, hexagonal crystals of hematite are found in the iron aventurine glazes (Bromberg 1915; Fraulini 1933; Dakhai, Orlova, and Mikhailenko 1999; Romero, Rincón, and Acosta 2004). This is the generic name for lead-free or low-lead glazes containing macroscopic laminar crystals, which cause a sparkling decorative effect. The effect, described as small glitters, probably originated in the seventeenth century in a furnace of Murano (Venice, Italy), when copper filings were accidentally spilled on molten glass, with such a surprising effect that it became part of factory production. The name “aventurine” comes from the Italian “a ventura”, which means “by chance”. In fact, Giovanni Darduin in a glassmakers’ book of recipes, known as the Darduin manuscript, says (149th recipe) that such a glass can be obtained more by chance than by the skill of the glassmakers (Zecchin 1986). The recipes used to obtain the aventurine effect have been very limited, confidential and restricted to the point of sometimes being forgotten over time. Darduin in the 149th recipe says to melt in a crucible 150 pounds of common glass and later to add 8 pounds of lead and tin oxides, 8 pounds of red copper oxide and, finally, 2.5 pounds of iron oxide. He recommends keeping the kiln at the same temperature for 8 or 10 h, then mix it again to homogenize the glass; close the door of the kiln, turn off the heat and let it cool naturally without touching it (Zecchin 2005).  $\text{Fe}_2\text{O}_3$  is the most reported oxide in literature as an effective generator of aventurine glazes (Lazău et al. 2013). In these glazes, the sparkling effect is due to the difference in the index of refraction between the crystalline and glassy phases. The macroscopic optical effect depends

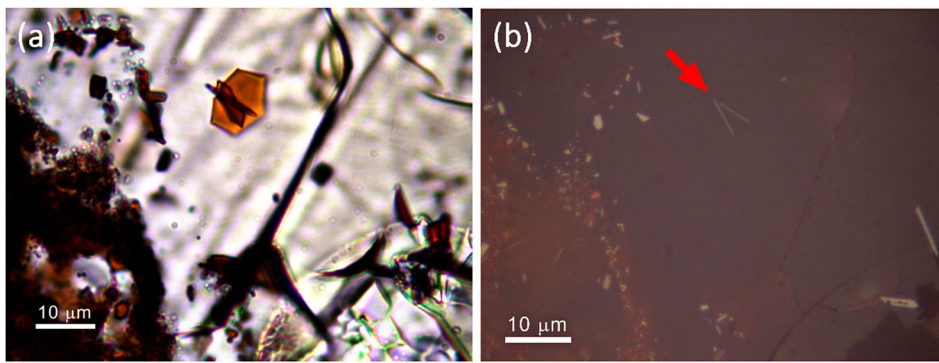


**Figure 7.** (a) OM image in PPL. Intergrowths of hexagonal crystals can be observed. (b) The same image as in picture (a) in reflected light. The growth habit of the hexagonal crystallites is missing and only two light laminar sections are visible.

on the size, volume fraction of crystallites,  $\text{Fe}_2\text{O}_3$  content and viscosity of melt (Levitskii 2001). References about the aventurine glazes composition can be found today in the literature (Shchiglova et al. 1996; Dakhai, Orlova, and Mikhailenko 1999; Levitskii 2001; Păcurariu et al. 2011; Lazău et al. 2013). In general,  $\text{Fe}_2\text{O}_3$  contents range from 10% to 30% by weight, and there are two groups of glazes, lead and boric, since a molten phase with low viscosity is required for the laminar crystal growth (Bromberg 1915). The alumina content (0.5–11 wt%) must be low and the proportion of  $\text{SiO}_2$  (30–60 wt%) is adjusted to obtain appropriate viscosity. The glazes can be obtained from glaze compositions consisting of natural raw materials or mixtures of frits and natural raw materials. The  $\text{Fe}_2\text{O}_3$  may be part of the frit or not, although in most compositions it is directly mixed into the glaze, owing to the disadvantages of synthesizing colored frits and because crystallization occurs more easily than if a homogeneous glass is used (Levitskii 2001). The thermal

cycle used to obtain these glazes usually consists of two stages: the first one for dissolving the metallic oxide in the melt, followed by slow controlled cooling that allows the laminar crystals to form or, otherwise, a certain dwell time at a lower temperature, where the crystalline growth rate is high. Cycle duration is very long, from 7–8 to 24 h (Dvornichenko and Matsenko 2000). In our case, the lead content is high while the iron content is low. In addition, the relatively small size of the hexagonal crystallites (few tens of micrometres) is due to a relatively fast cooling which also causes the formation of skeletal melanotekite crystals in the sample 9703 (Di Febo et al. 2017). For these reasons, the decorative effect in the coating is missing. However, some fragments of the Taches Noires wares, observed under stereomicroscope, show a golden shade which is more evident on the manganese brown decorated areas. In fact, these are the samples which are richer in hexagonal crystallites because the manganese can act as a nucleating agent for the growth of

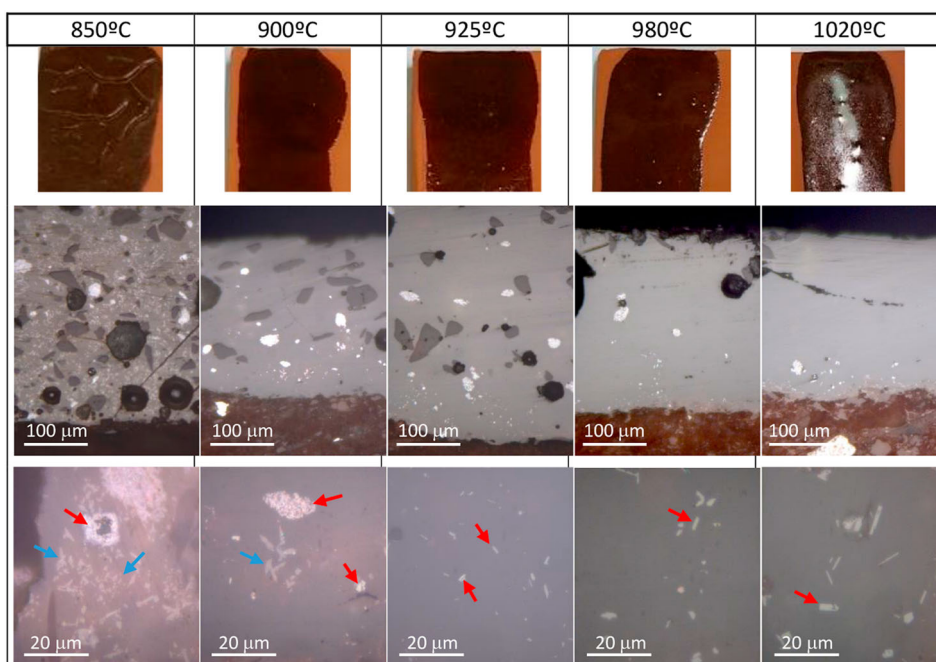


**Figure 8.** Above: reproductions of the glaze composition of the sample 9703 at different temperatures. Below: OM images of the glazes in reflection mode. Melanotekite crystals are marked in blue arrows and hematite in red arrows.

hexagonal planar hematite crystallites. Studies of aventurine glazes demonstrated that the introduction of about 3% MnO in an iron rich melt leads to an increase of 10–15% on the volume fraction of hematite crystals (Romero, Rincón, and Acosta 2004). Although an iron content of about 4–6 wt%, such as found in our ceramic glazes, may appear low as compared to the values expected in aventurine glazes, it is sufficient to generate a situation of iron oversaturation that leads to the precipitation of hematite. The rate of the crystals increases with increasing supersaturation. Then, we can observe individual crystals or intergrowths of hexagonal crystals (Figures 7(a,b)). The lamellar shape of the crystals is presumably determined by the growth conditions: increased melt viscosity and a high degree of melt oversaturation with iron oxide (Levitskii 2001). Taking into account the SEM–FIB observations above, the hematite crystallites were mostly found inside the glaze. This evidence is in good agreement with the literature data on aventurine glazes showing an increase in the amount of crystallites across the

entire thickness of the coating up to a depth of about 100  $\mu\text{m}$  (Levitskii 2001).

Finally, in order to determinate the thermal range at which hematite was formed, we replicated under laboratory-controlled conditions the same glaze composition than that of the sample 9703 (Figure 8) using chemical reagents (60.8 wt% of minium – $\text{Pb}_3\text{O}_4$ –, 32.6 wt% of quartz, 4.3 wt% of kaolin, 5.53 wt% of  $\text{Fe}_2\text{O}_3$ , 1.34 wt% of wollastonite and 1 wt % of talc). The glazes were applied over a ceramic flat surface made with an illitic–kaolinitic clay containing 6%  $\text{Fe}_2\text{O}_3$  and fired at different temperatures: 850°C, 900°C, 925°C, 950°C, 980°C and 1050°C. Hematite in association with melanotekite are found in those replications fired at 850°C, although the glaze appears not fully molten. Moreover, we observe clusters resembling the grains of hematite originally present in the glaze mixture and hematite and melanotekite recrystallized around them. At 900°C the glaze is completely molten and melanotekite and hematite are also present (Figure 9). Above 920°C melanotekite appears

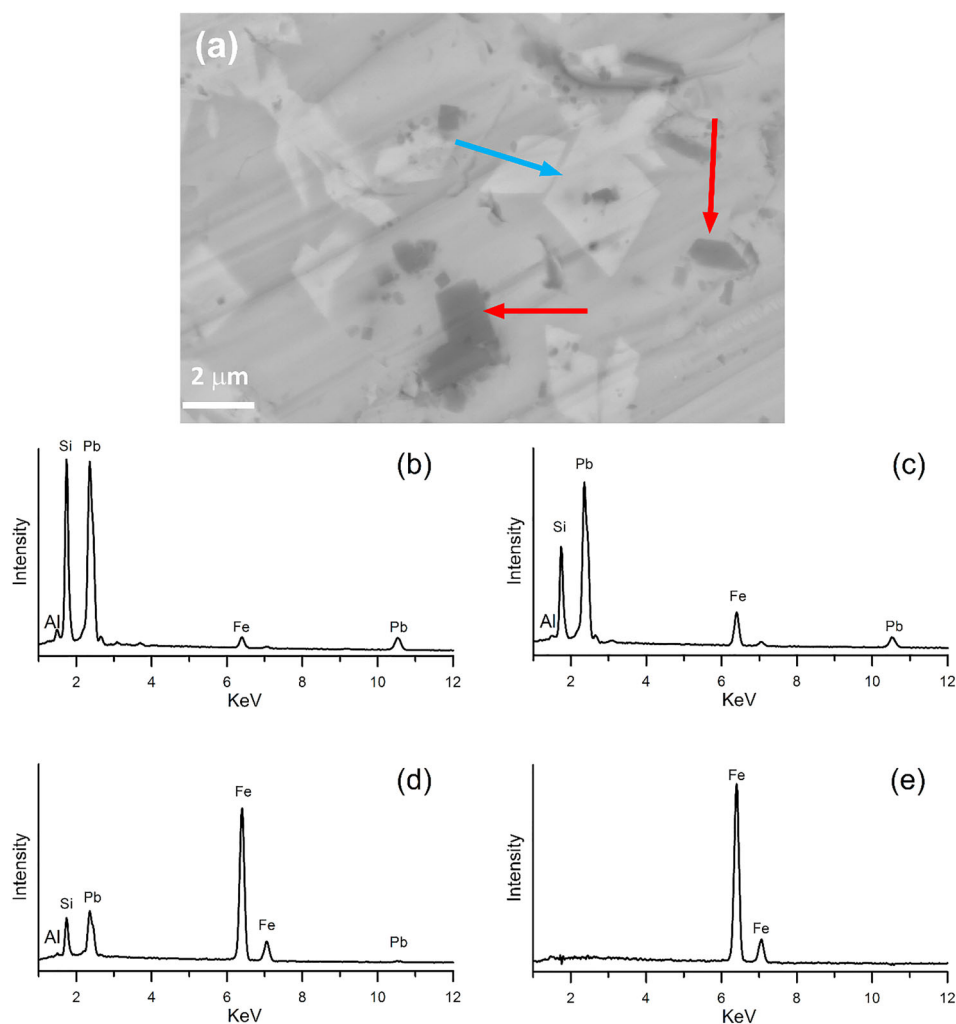


**Figure 9.** (a) SEM backscattering image of the glaze reproduction of the sample 9703 fired at 900°C. Light crystals correspond to melanotekite (blue arrow) and dark crystals correspond to hematite (red arrows) are visible. (b) EDS spectrum of the glaze. (c) EDS spectrum of melanotekite crystals (blue arrow). (d) EDS spectrum of hematite crystal (central red arrow). (e) EDS spectrum of hematite crystal (central red arrow) subtracting the glaze spectrum.

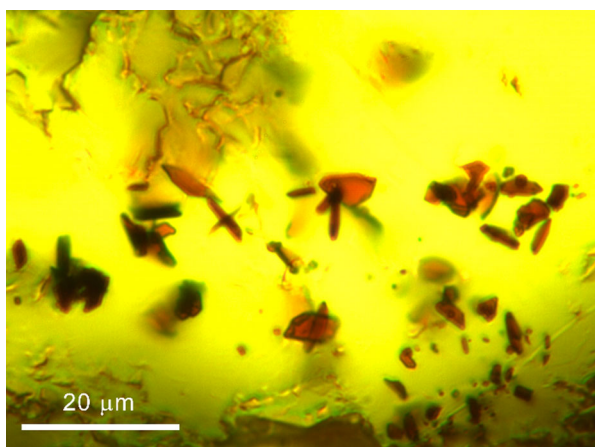


**Figure 10.** OM images in PPL. Glaze reproduction of the sample 9703 fired at 925°C. Only hematite crystallites can be observed.

completely absent. On the contrary, hematite crystals growing at the ceramic body–glaze interface appear in all replicas and these are larger and thicker for those replicas fired at higher temperature. These results demonstrate that melanotekite and hematite nucleate and grow during the heating. Melanotekite is formed by the reaction between lead oxide, quartz and iron oxide during the melting. At temperatures over 900°C, melanotekite is dissolved in the melt (Figure 10). Hematite hexagonal crystals are preferentially formed at the ceramic–glaze interface where nucleating sites exist. The original hematite grains appear more dissolved at higher temperatures. At 950–1020°C few recrystallized grains of the original hematite grains remain and bigger hexagonal hematite crystals are observed near the interface. The presence of hematite in association with melanotekite in the sample 9703 from Jouques, suggests that it was fired at about 900°C and below 925°C.

## 5. Conclusions

This case study shows how a multi-analytical approach is crucial to identify the hexagonal neo-formed crystallites of hematite in ceramic lead glazes. In particular, the optical observation in PPL was able to localize the micro-crystallites in the glaze and show their distribution and growth habits, while SR- $\mu$ XRD carried out directly on the thin section was able to identify their nature. Taking into account that the hexagonal habits of crystallites were never found on the polished surfaces of the glazes, the optical observation in PPL is a very powerful tool to correlate the hexagonal morphologies of these crystallites to thin cross sections that can be observed in the SEM. Based on the experimental data, the presence of hematite in association with melanotekite in high lead glazes is indicative of low firing temperatures (<925°C), while the presence of only hematite seems to be a fingerprint of higher temperatures (>925°C).

As noted in this work, the hexagonal neo-formed hematite crystals found in our ceramic lead glazes are also a typical feature of the aventurine glazes. Although these crystals have been observed in archaeological ceramics of different provenance and chronology, their presence is more the chance result of the interaction between paste and glaze of a specific composition than a deliberate decorative effect. In fact, the presence of these crystals can be noted only by petrographic observations, while on the brown decorations using a stereomicroscope. However, also on the brown decorations, the sparkling effect is limited. The difficulty in obtaining the aventurine effect, together with the clear dependence on the glaze composition and the firing cycle led to an unreliability of duplicating the results. The method of the temperature treatment is important as well as the composition of the body to which the glaze is applied. The chief difficulty in producing aventurine is not in the nucleation but is in the enlargement and dispersion of the crystals. This process occurs during a very slow cooling period. The glass must be cooled slowly until it reaches ambient temperature. It is during this time that the crystals growth becomes almost visible to the naked eye.

## Acknowledgement

Roberta Di Febo is grateful to the UVICUCC Scholarship Program, awarded by University of Vic, Central University of Catalonia. The authors are grateful to the project MAT2016-77753-R, 2017-2019 funded by the Ministerio de Ciencia e Innovación (Spain), the ALBA Synchrotron Light Facility 2014060905 (BL04) and the Generalitat de Catalunya project 2014 SGR 00581 (T.P.), 2014 SGR1585 (J.M. and R.D.F.).

## Disclosure statement

No potential conflict of interest was reported by the authors.

## Notes on contributors

**Roberta Di Febo** completed her Ph.D. in Archaeological Science at the University of Barcelona (Spain) in 2016. In 2018, she will conclude her second Ph.D. in Archaeometry at the University of Vic (Spain). The use of thin section petrography in combination with other analytical tools is the focus of her interest in ceramic glazes.

**Judit Molera** born in Barcelona July 1966. Ph.D. in Geology at the Universitat de Barcelona (UB) in 1996. Assistant professor in the Department of Crystallography and Mineralogy (UB) 1990–2004. Researcher RyC in the University of Girona (UdG) 2004–2007 and Professor of the University of Vic-Central University of Catalonia (UVIC-UCC) since 2007. Expert in Ceramic Materials mainly devoted to the study of crystals developed in glazes and decorations of ancient ceramics using micro-XRD, optical and electron microscopy. 59 papers published. H index 21, 1289 cites (Scopus).



**Trinitat Pradell** born in Barcelona march 1961. Ph.D. in Applied Physics at the Universitat de Barcelona in 1992. Full Professor in Applied Physics in the Department of Physics of the Universitat Politècnica de Catalunya (Barcelona-Tech) since 2010. Research projects in Materials Science mainly devoted to the study of amorphous and nanocrystalline materials and Historical and Artistic materials, specially of ceramic, glass, glaze technology with particular input to glass decorations, enamels and paintings. Over 125 papers published. H index from the WOS, 21. 1517 cites without self citations.

**Oriol Vallcorba** PhD in Chemistry from the Universitat Autònoma de Barcelona in 2010. Post-doc in the Materials Science and Powder Diffraction beamline at the ALBA synchrotron. Since 2014, his research is focused on the development of methodologies for crystal structure studies from diffraction techniques, specially polycrystalline x-ray diffraction and microdiffraction. 34 publications indexed in the WOS (H-index 8).

**Claudio Capelli** born in Savona (Italy) december 1963. Ph.D. in Earth Sciences in 1993, University of Genova. Researcher at the Department for the Earth, Environment and Life Sciences (DISTAV) of the University of Genova. External collaborator to the Centre Camille Jullian (Aix-Marseille Université/CNRS, UMR 7299) of Aix-en-Provence (France). Main research topic: archaeometry of Prehistoric to post-Medieval Mediterranean pottery by means of mineralogical and petrographic methods. Over 260 papers published.

## ORCID

Roberta Di Febo  <http://orcid.org/000-0002-1102-8231>

Judit Molera  <http://orcid.org/0000-0003-3116-0456>

Trinitat Pradell  <http://orcid.org/0000-0002-8720-5492>

Oriol Vallcorba  <http://orcid.org/0000-0001-6499-7688>

Claudio Capelli  <http://orcid.org/0000-0003-1318-880X>

## References

- Amouric, H., and L. Vallauri. 1993. La fabrique de Villemus. In *Un goût d'Italie, Céramiques et céramistes italiens en Provence du Moyen Âge au XXème siècle*, Catalogue Exposition, Narration, Aubagne, 118–120.
- Beltrán de Heredia Bercero, J., C. Capelli, R. Di Febo, M. Madrid i Fernández, and J. Buxeda i Garrigós. 2015. Imitaciones de cerámicas Taches Noires en Barcelona en el siglo XVIII. Datos arqueológicos y arqueométricos. In *Actas do X Congresso Internacional A Cerâmica Medieval no Mediterrâneo- Silves 2012-*, Camera Municipal de Silves & Campo Arqueológico de Mértola, 613–618.
- Blake, H. 1981. "Pottery Exported from Northwest Italy Between 1450 and 1830: Savona, Albisola, Genoa, Pisa, and Montelupo." In *Archaeology and Italian Society. Prehistoric, Roman and Medieval Studies*, edited by G. Barker, and R. Hodges, 99–124. Oxford: BAR International Series 102.
- Bromberg, N. 1915. "A Study of Compositions Suitable for Aventurine Glazes." (Thesis (MS)). University of Illinois. <http://hdl.handle.net/2142/53956>.
- Cameirana, A. 1970. La terraglia nera ad Albisola all'inizio dell'800. In *Atti III Convegno Internazionale della Ceramica 1969*, Centro Ligure per la Storia della Ceramica, Firenze, 63–95.
- Cameirana, A. 1977. La ceramica albisolese a Taches Noires. In *Atti del X Convegno Internazionale della Ceramica 1976*, Centro Ligure per la Storia della Ceramica, Firenze, 277–293.
- Capelli, C., R. Di Febo, H. Amouric, R. Cabella, and L. Vallauri. 2017. Importazioni e imitazioni locali di ceramica a Taches noires in Provenza nel XVIII-XIX secolo. Dati archeologici e archeometrici. In *Atti IL Convegno Internazionale della Ceramica 2016*, Centro Ligure per la Storia della Ceramica, Firenze.
- Capelli, C., T. Mannoni, and R. Cabella. 2007. Analisi archeometriche e Archeologiche integrate sulla ceramica inventriata da fuoco dal Palazzo Ducale di Genova (XII-XIII sec.). In *Atti XXXIX Convegno Internazionale della Ceramica 2006*, Centro Ligure per la Storia della Ceramica, Firenze, 7–16.
- Capelli, C., F. Richez, L. Vallauri, R. Cabella, and R. Di Febo. 2013. L'épave du Grand Congloué 4: Caractérisation archéologique et archéométrique d'un lot de céramiques à Taches Noires de Albisola-Savona. In *Atti XLV Convegno Internazionale della Ceramica 2012*, Centro Ligure per la Storia della Ceramica, Firenze, 7–16.
- Casadio, F., C. Daher, and L. Bellot-Gurlet. 2016. "Raman Spectroscopy of Cultural Heritage Materials: Overview of Applications and New Frontiers in Instrumentation, Sampling Modalities, and Data Processing." *Topics in Current Chemistry* 374: 1434. doi:10.1007/s41061-016-0061-z.
- Clark, R. J. H., and M. L. Curri. 1998. "The Identification by Raman Microscopy and X-ray Diffraction of Iron-Oxide Pigments and of the Red Pigments Found on Italian Pottery Fragments." *Journal of Molecular Structure* 440: 105–111.
- Colomban, P., and C. Truong. 2004. "Non-destructive Raman Study of the Glazing Technique in Lustre Potteries and Faience (9th–14th Centuries): Silver Ions, Nanoclusters, Microstructures, and Processing." *Journal of Raman Spectroscopy* 35: 195–207.
- Dakhai, S., L. A. Orlova, and N. Y. Mikhailenko. 1999. "Types and Compositions of Crystalline Glazes." *Glass and Ceramics* 56 (5): 177–180.
- De Faria, D. L. A., and F. N. Lopes. 2002. "Natural Hematite or Heated Goethite: Can Raman Microscopy Differentiate Them?" In *XVIIIth International Conference on Raman Spectroscopy*, edited by J. Mink, G. Jalsovszhy, and G. Keresztury, 825–826. New York: Wiley.
- De Faria, D. L. A., V. Silva, and M. T. de Oliveira. 1997. "Raman Microspectroscopy of Some Iron Oxides and Oxyhydroxides." *Journal of Raman Spectroscopy* 28: 873–878.
- Di Febo, R. 2016. "La ceràmica de Barcelona entre els segles XIII i XVIII a través de la seva caracterització arqueomètrica. El paper de l'anàlisi petrogràfica." (Doctoral diss.). University of Barcelona, Barcelona. <http://diposit.ub.edu/dspace/handle/2445/>.
- Di Febo, R., J. Molera, T. Pradell, O. Vallcorba, and C. Capelli. 2017. "Thin Section Petrography and SR- $\mu$ XRD for the Identification of Micro-crystallites in the Brown Decorations of Ceramic Lead Glazes." *European Journal of Mineralogy*, doi:10.1127/ejm/2017/0029-2638.
- Dvornichenko, I. N., and S. V. Matsenko. 2000. "Production of Iron-containing Crystalline Glazes." *Glass and Ceramics* 57 (1–2): 67–68.
- Fraulini, F. 1933. "Aventurine Glazes." (Bachelors Theses). Missouri School of Mines and Metallurgy, Missouri. [http://scholarsmine.mst.edu/bachelors\\_theses/309](http://scholarsmine.mst.edu/bachelors_theses/309).

- Gómez, A., C. Gil, R. Di Febo, and J. Molera. 2015. Casa Convalescència (Vic, Osona): Aproximació arqueològica i arqueomètrica a un conjunt de vasos ceràmics del segle XVIII. In *III Jornades d'Arqueologia de la Catalunya Central*, Roda de Ter, 70–81.
- Howell, G., M. Edwards, and P. Vandenabeele. 2016. "Raman Spectroscopy in Art and Archaeology." *Philosophical Transaction of the Royal Society A* 374 (2082), doi:10.1098/rsta.2016.0052.
- Lazău, I., S. Borcănescu, C. Păcurariu, and C. Vancea. 2013. "Kinetic Study of the Non-isothermal Crystallization Process of Hematite in Ceramic Glazes Obtained from CRT Wastes." *Journal of Thermal Analysis and Calorimetry* 112 (1): 345–351. doi:10.1007/s10973-012-2736-1.
- Levitskii, I. A. 2001. "Mechanism of Phase Formation in Aventurine Glaze." *Glass and Ceramics*, 58 (5): 223–226. doi:10.1023/A:1012351301045.
- Păcurariu, C., R. I Lazău, I. Lazău, D. Tița, and D. Dumitrel. 2011. "Nonisothermal crystallization kinetics of some aventurine decorative glaze." *Journal of Thermal Analysis and Calorimetry* 105: 1130–0.
- Poole, A. B., and I. Sims. 2015. *Concrete Petrography: A Handbook of Investigative Technique*. 2nd ed. CRC Press.
- Romero, M., J. Rincón, and A. Acosta. 2004. "Development of Mica Glass-Ceramic Glazes." *Journal of the American Ceramic Society* 87: 819–823. doi:10.1111/j.1551-2916.2004.00819.x.
- Shchiglova, M. D., T. V. Babenko, S. G. Polozhai, and V. M. Svistun. 1996. "Mechanism of Aventurine Formation in Copper-containing Alkali-lead Silicate Glass." *Glass and Ceramics* 53 (1–2): 14–17.
- Smith, G. D., and R. J. H. Clark. 2001. "Raman Microscopy in Art History and Conservation Science." *Reviews in Conservation* 2: 92–106.
- Tite, M. S., I. Freestone, R. Mason, J. Molera, M. Vendrell-Saz, and N. Wood. 1998. "Lead Glazes in Antiquity – Methods of Production and Reasons for Use." *Archaeometry* 40 (2): 241–260.
- Zecchin, L. 1986. *Il Ricettario Darduin, un codice vetrario del Seicento, trascritto e commentato*. Stazione Sperimentale del Vetro e Arsenale, Venezia.
- Zecchin, L. 2005. "La Pasta Venturina, Vetro Speciale Muranese." *Journal of Glass Studies* 47: 93–106.